Eliashberg Analysis of Tunneling Experiments: Support for the Pairing Glue Hypothesis in Cuprate Superconductors

O. Ahmadi, L. Coffey, and J. F. Zasadzinski
Physics Department, Illinois Institute of Technology, Chicago, Illinois 60616, USA

N. Miyakawa
Department of Applied Physics, Tokyo University of Science, Shinjuku Ku, Tokyo 1628601, Japan

L. Ozyuzer
Department of Physics, Izmir Institute of Technology, TR-35430, Izmir, Turkey
(Received 29 September 2010; published 22 April 2011)

Evidence for the validity of the pairing glue interpretation of high temperature superconductivity is presented using a modified Eliashberg analysis of experimental superconductor-insulator-superconductor (SIS) tunneling data in $B_2Sr_2CaCu_2O_8$ (Bi2212) over a wide range of doping. This is accomplished by extracting detailed information on the diagonal and anomalous contributions to the quasiparticle self-energy. In particular, a comparison of the imaginary part of the anomalous self-energy $\mathrm{Im}\Phi(\omega)$ and the pairing glue spectral function $\alpha^2F(\omega)$ used in the model is consistent with Hubbard model simulations in the literature. In addition, the real part of the diagonal self-energy for optimal doped Bi2212 bears a strong resemblance to that obtained from photoemission experiments.

DOI: 10.1103/PhysRevLett.106.167005 PACS numbers: 74.45.+c, 74.20.Mn, 74.72.−h

The nature of the mechanism leading to high temperature superconductivity in the copper-oxide materials remains unresolved, 24 years after their discovery. The close proximity of the superconducting and antiferromagnetic insulator phases in the phase diagram of these materials has led to speculation that the superconducting mechanism originates in the antiferromagnetic properties of the copper-oxide layers of these compounds.

A pairing mechanism based on a low frequency spectrum of antiferromagnetic spin fluctuations of the high-T_c materials is referred to as the pairing glue mechanism, and has been the subject of extensive theoretical studies of the Hubbard and t-J Hamiltonians [1–4]. Such studies reveal retardation effects in the pairing self-energy similar to the frequency dependent gap features found in conventional electron-phonon coupled superconductors. The imaginary part of the electronic spin susceptibility, $\mathrm{Im}\chi(q, \omega)$, plays a central role in the pairing mechanism in this scenario.

The validity of the pairing glue mechanism has been challenged by a very different physical picture of the origin for superconductivity in the copper oxides [5]. The pairing mechanism in this latter approach originates in high energy electronic scattering, on the energy scale of the superexchange constant $J \simeq t^2/U$, and views the high-T_c state as emerging, with doping away from half filling, from a Mott insulator ground state of resonant valence bond, spin-singlet, electron pairs. In this picture, the interactions are instantaneous and therefore any attempt to explain electron spectroscopies with retardation effects, as found in Eliashberg models, would be expected to fail.

Theoretical studies have demonstrated the ability of a mechanism mediated by antiferromagnetic spin fluctuations to generate the correct d-wave superconducting gap symmetry [6,7], as well as other notable properties such as a dip feature observed in angle resolved photoemission spectroscopy (ARPES) and tunneling experiments [8–10]. This latter feature can be connected to the so-called resonance mode of the antiferromagnetic spin fluctuation spectrum measured in inelastic neutron scattering (INS) [11,12].

In the present work, new evidence for the pairing glue mechanism is presented from an analysis of experimental superconductor-insulator-superconductor (SIS) tunneling conductance data on $B_2Sr_2CaCu_2O_8$ Bi2212 using a modified d-wave Eliashberg model [13]. Self-consistency is demonstrated as the bosonic spectral weight function that fits the spectral dip feature also generates the correct gap value. Our fit of optimal doped Bi2212 shows that this analysis can generate the anomalous negative dI/dV observed in experiment. This Eliashberg based analysis yields both the diagonal and off-diagonal (anomalous) complex valued self-energy functions.

The results add significant new insights to previous modeling of experimental data on Bi2212 [14,15] which provided a theoretical justification for superconducting gap and bosonic mode energies extracted from the SIS tunneling experiments for different levels of doping in Bi2212 [16]. In Refs. [14,15] the emphasis was on a comparison between the real part of the diagonal self-energy $\Sigma(\omega)$ [$\Sigma(\omega) = \omega[1 - Z(\omega)]$] extracted from modeling tunneling data with a related quantity extracted from a memory

function model analysis of optical conductivity [17]. The conclusion was the continued key role of the bosonic resonance mode in the mechanism for the overdoped superconducting state, contrary to what the optical conductivity measurements seemed to indicate [17]. With the new results for $\mathrm{Re}\Sigma(\omega)$ for optimal doped Bi2212, we are also now able to compare directly with the same quantity obtained by ARPES, and we find a striking correspondence which justifies the assumptions built into our analysis.

Here we demonstrate the ability of the Eliashberg analysis to explain previously unpublished, subtle, features in the experimental SIS Bi2212 break junction tunneling conductances. In addition, the frequency dependent imaginary part of the off-diagonal, pairing self-energy $\Phi(\omega)$ is extracted from the experimental measurements. In the present work, $\Phi(\omega)$ is related to the d-wave superconducting gap by $\Delta(\omega)\cos(2\phi) = [\Phi(\omega)/Z(\omega)]\cos(2\phi)$. The results for $\Phi(\omega)$ of the present work can then be compared with the same quantity from the numerical and theoretical calculations [1,2].

A states conserving normalization of low leakage SIS conductance spectra [18] is used in this analysis. We take advantage of a number of studies [19–21] that show clearly that the normal state conductance is a smoothly varying function which merges with the superconducting conductance for voltages just beyond that of the hump in the dip or hump spectral feature. Published SIS tunneling conductances [16] have been normalized by generating a normal state conductance which smoothly interpolates between the positive and negative high bias superconducting data just beyond the hump voltage. An example of the superconducting data for optimal doped Bi2212 and generated normal state conductance is shown in the top inset of Fig. 1.

The modified Eliashberg model used to analyze the experimental tunneling conductance data from Bi2212 junctions is given by the coupled equations for $Z(\omega)$ and $\Delta(\omega)$:

$$\omega Z(\omega) = \omega - \int_0^\infty d\omega' c_Z \omega' K_-(\omega', \omega) \times \int_0^{2\pi} \frac{d\phi'}{2\pi} \mathrm{Re} \frac{1}{\sqrt{\omega'^2 - \Delta^2(\omega')\cos^2(2\phi')}}, \quad (1)$$

$$\Delta(\omega) = \frac{1}{Z(\omega)} \int_0^\infty d\omega' c_\Delta \Delta(\omega') K_+(\omega', \omega) \times \int_0^{2\pi} \frac{d\phi'}{2\pi} \mathrm{Re} \frac{\cos^2(2\phi')}{\sqrt{\omega'^2 - \Delta^2(\omega')\cos^2(2\phi')}}, \quad (2)$$

$$K_\pm(\omega', \omega) = \int_0^\infty d\omega'' \alpha^2 F(\omega'') \times \left(\frac{1}{\omega + \omega' + \omega'' + i\delta} \mp \frac{1}{\omega - \omega' - \omega'' + i\delta} \right). \quad (3)$$

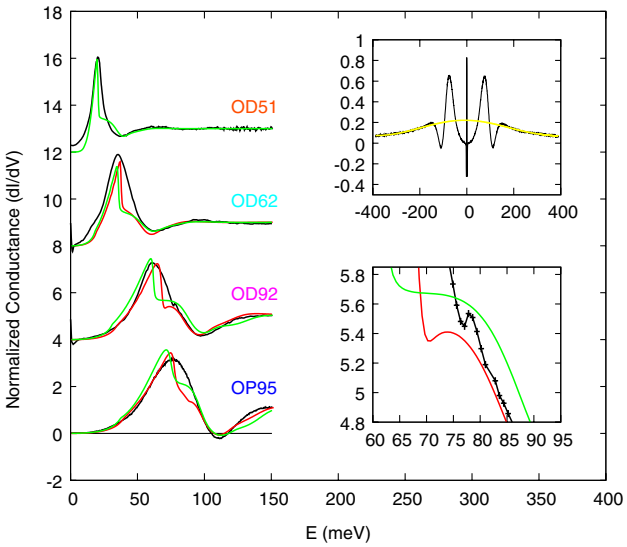

FIG. 1 (color online). Comparison of normalized SIS break junction tunneling conductance (black curves) and d-wave Eliashberg fits for four junctions with $\Delta = 10.5$ meV (OD51), 17.5 meV (OD62), 31 meV (OD92), and 38 meV (OPT95). The (c_Z, c_Δ) values used for the light gray (green) curves, for example, are $(0.14, 0.9)$, $(0.15, 0.78)$, $(0.2, 0.8)$, and $(0.2, 0.83)$, and the directional tunneling (a, b) values used are $(0.08, 1.8)$, $(0.28, 0.7)$, $(0.28, 0.7)$, and $(0.2, 0.87)$, respectively. Upper inset: Experimental optimal doped superconducting and normal state normalization curve (see text). Lower inset: An enlargement of the small feature on the main conductance peak for the case of $\Delta = 31$ meV (OD92).

Equations (1) and (2) are based on a pairing interaction given by $\{c_Z + c_\Delta \cos[2(\phi - \phi')]\}\alpha^2 F(\omega)$ [22], where the frequency spectrum of the pairing boson is given by $\alpha^2 F(\omega)$ (see the inset of Fig. 3). The fits shown in Fig. 1 demonstrate the capability of the pairing glue approach to explain quantitatively the value of the maximum superconducting gap Δ (from the position of the peak in the SIS conductances) as well as the position and magnitude of the prominent dip feature in the conductance over a wide range of doping. The position of the dip is given, to a good approximation, by $2\Delta + \Omega_M$, where Ω_M is the position of the main peak in the $\alpha^2 F(\omega)$. Figure 1 shows fits of four experimental SIS tunneling conductances on Bi2212 over a wide range of doping from optimal to overdoped, with the fits for OD62, OD92, and OPT95 using two different sets of Ω_M values [dark gray (red) and light gray (green) dots in the inset of Fig. 2]. The OD51 ($\Delta = 10.5$ meV) fit has been published before [15].

A relatively narrow range of Ω_M values, shown in the inset of Fig. 2, provides acceptable fits, with the smaller values of Ω_M consistent with the estimates in Fig. 3 of Ref. [16], and the larger values obtained using the $5.4 k_B T_c$ scaling relation obtained from INS measurements [11,12]. The Ω_M values display a clear correlation with T_c, and are consistent with Ω_M being the resonance mode. The small difference between the Ω_M values of Ref. [16] and the

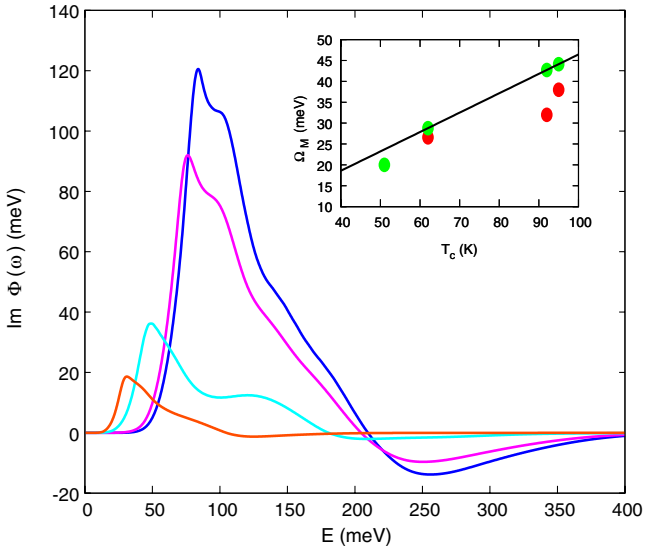

FIG. 2 (color online). $\mathrm{Im}\Phi(\omega)$ extracted from the fits of the junctions of Fig. 1 [light gray (green) curves]. Inset: The Ω_M values used for the light gray (green) curves of Fig. 1 are indicated by the light gray (green) dots, and those for the dark gray (red) curves of Fig. 1 by the dark gray (red) dots. The solid line denotes the INS derived $5.4k_BT_c$ scaling relation.

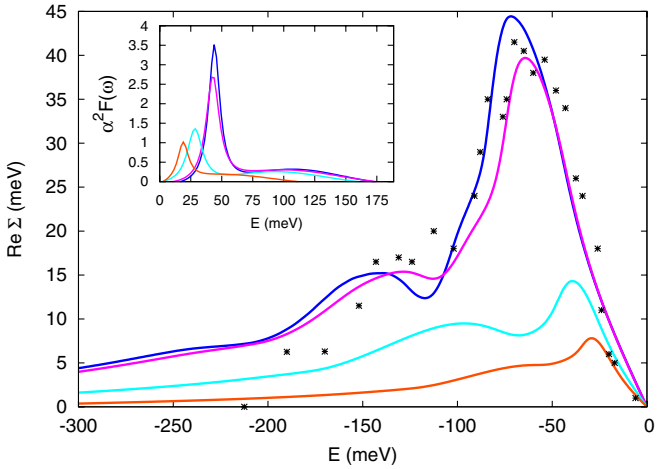

FIG. 3 (color online). The $\mathrm{Re}\Sigma(\omega)$ extracted from the four fits shown in Fig. 1 [light gray (green) curves]. The curves are plotted as a function of negative frequency for ease of comparison with the self-energy extracted from ARPES (black crosses, Ref. [26]). Inset: The four $\alpha^2F(\omega)$ spectra used in the light gray (green) curve fits in Fig. 1.

values from INS may arise from surface inhomogeneity in doping to which tunneling is sensitive, and which could lead to small differences with bulk INS measurements of the mode energy. The Ω_M values are used as a fixed, independent input parameter in the Eliashberg analysis, determining the energy scale for all of the other features in the SIS conductance curves. A notable feature of the experimental data is the large ratio of the height of the main conductance peak to the high bias voltage background. This is typically close to or greater than 3 (see Fig. 1), and is reproduced in the fitting by interpreting it as evidence of directional tunneling. A tunneling matrix element $a + b\cos^2(2\phi)$ is used to incorporate directional tunneling in each of the two quasiparticle density of states functions used in the convolution that leads to the model SIS tunneling conductances [23].

The overall agreement between the model and experiment in Fig. 1 is excellent although the model displays a sharper downturn in the conductance for energies just beyond the peak. Some junction data, as shown in the lower inset of Fig. 1 from curve OD92, display fine structure which is quite similar to a weak secondary feature arising in the model due to strong coupling effects. Other junctions display a smoother conductance peak. We argue that fine structure would easily be washed out by any inhomogeneities in the superconducting gap value expected to be found over the relatively large junction areas of these break junctions.

A second unusual feature occurs at optimal doping where the measured SIS conductance becomes slightly negative in the vicinity of the minimum of the dip feature. The Eliashberg based model can reproduce this behavior (as seen in the bottom curve of Fig. 1). Such a feature is a stringent test for other interpretations of the conductance dip, for example, pseudogap or charge density wave gaps, which, to our knowledge, can never lead to a negative dynamic conductance. Figure 2 shows the frequency dependence of the imaginary part of the anomalous self-energy [$\mathrm{Im}\Phi(\omega)$] with the corresponding $\alpha^2F(\omega)$ curves used in these fits shown in the inset of Fig. 3. The evolution of $\alpha^2F(\omega)$ from optimal to the overdoped results in the main spectral weight peak shifting to lower energies and becoming less pronounced with respect to the high energy background, which itself covers a reduced energy range as doping increases. The $\alpha^2F(\omega)$ in Fig. 3 resemble bosonic spectra obtained from an analysis of optical conductivity experiments [24]. The temperature dependence of the bosonic spectrum has also been extracted by a different group using an Eliashberg analysis of optical conductivity measurements [25].

In Fig. 2, the peak in the $\mathrm{Im}\Phi(\omega)$ is shifted relative to the peak in $\alpha^2F(\omega)$ by the calculated maximum gap value. This is to be expected in an Eliashberg calculation. In the work of Ref. [2], this same effect arises in the overdoped case and is shown in Fig. 4 of Ref. [2] for the doping parameter $\delta \geq 0.15$ and $U/t = 8$. In the results for underdoped ($\delta \leq 0.15$) in Ref. [2], an additional contribution to the gap in the density of states, presumably the pseudogap, arises which changes this relation as shown in Fig. 4 of Ref. [2]. We, however, are always dealing with the optimal or overdoped regime.

In Fig. 3, we assume that the $\mathrm{Re}(\Sigma(\omega))$ extracted from the Eliashberg analysis is antisymmetric about $\omega = 0$ to plot the $\mathrm{Re}(\Sigma(\omega))$ along the negative ω axis. In this way,

we can compare the results of the present analysis with $\mathrm{Re}(\Sigma(\omega))$ extracted from an analysis of the ARPES momentum distribution curve in Bi2212 below T_C. The correspondence between the magnitude and shape of the self-energy extracted from the present analysis of the SIS tunneling data for the optimal doped case, and that obtained from ARPES data [26], lends more support to the validity of a pairing glue Eliashberg picture of the pairing mechanism in Bi2212, as well as the assumption in the present work that $Z(\omega)$ is independent of angle ϕ. The slope of the $\mathrm{Re}(\Sigma(\omega))$ at $\omega = 0$ can be used to quantify an effective superconducting coupling strength λ, yielding values 0.22 ($\Delta = 10.5$ meV), 0.3 ($\Delta = 17.5$ meV), 0.46 ($\Delta = 31$ meV), and 0.46 ($\Delta = 38$ meV). These trends can be compared with the quantity $2\int \alpha^2 F(\omega) d\omega/\omega$, which is used in s-wave strong coupling theory as a measure of the coupling constant. This results in 1.58 ($\Delta = 10.5$ meV), 1.78 ($\Delta = 17.5$ meV), 2.12 ($\Delta = 31$ meV), and 2.27 ($\Delta = 38$ meV). These latter, admittedly crude, estimates of λ compare favorably with similar estimates shown in Table I of Ref. [24] for optimal and overdoped Bi2212.

To summarize, we have demonstrated that tunneling data in Bi2212 can be fitted using a d-wave Eliashberg formalism over a wide doping range where the superconducting gap changes nearly by a factor of 4. Self-consistency is achieved as the $\alpha^2 F(\omega)$ which fits the spectral dip also leads to the correct value of the superconducting gap. New results for the fit to optimally doped Bi2212 show that the anomalous negative dynamic conductance measured at the dip minimum is easily explained within this strong coupling scenario. Other interpretations of the spectral dip (for example, charge density wave gaps) are unlikely to reproduce a negative conductance. A direct comparison of the diagonal self-energy in optimal doped Bi2212 to that found in ARPES along the nodal direction shows good agreement. Recent work [27] incorporating a spin susceptibility derived from INS experiments has also been used in a detailed analysis of YBCO ARPES data.

[1] T. A. Maier, D. Poilblanc, and D. J. Scalapino, Phys. Rev. Lett. **100**, 237001 (2008).

[2] B. Kyung, D. Senechal, and A. M. S. Tremblay, Phys. Rev. B **80**, 205109 (2009).

[3] T. A. Maier, A. Macridin, M. Jarrell, and D. J. Scalapino, Phys. Rev. B **76**, 144516 (2007).

[4] E. Khatami, A. Macridin, and M. Jarrell, Phys. Rev. B **80**, 172505 (2009).

[5] P. W. Anderson, Science **316**, 1705 (2007).

[6] N. E. Bickers, D. J. Scalapino, and S. R. White, Phys. Rev. Lett. **62**, 961 (1989).

[7] P. Monthoux and D. Pines, Phys. Rev. Lett. **69**, 961 (1992).

[8] T. Dahm, Phys. Rev. B **53**, 14051 (1996).

[9] M. Eschrig and M. R. Norman, Phys. Rev. Lett. **85**, 3261 (2000).

[10] M. Eschrig, Adv. Phys. **55**, 47 (2006).

[11] L. Capogna, B. Fauque, Y. Sidis, C. Ulrich, Ph. Bourges, S. Pailhes, A. Ivanov, J. L. Tallon, B. Liang, C. T. Lin, A. I. Rykov, and B. Keimer, Phys. Rev. B **75**, 060502(R) (2007).

[12] B. Fauque, Y. Sidis, L. Capogna, A. Ivanov, K. Hradil, C. Ulrich, A. I. Rykov, B. Keimer, and P. Bourges, Phys. Rev. B **76**, 214512 (2007).

[13] E. Schachinger and J. P. Carbotte, J. Phys. Stud. **7**, 209 (2003).

[14] J. F. Zasadzinski, L. Coffey, P. Romano, and Z. Yusof, Phys. Rev. B **68**, 180504 (2003).

[15] J. F. Zasadzinski, L. Ozyuzer, L. Coffey, K. E. Gray, D. G. Hinks, and C. Kendziora, Phys. Rev. Lett. **96**, 017004 (2006).

[16] J. F. Zasadzinski, L. Ozyuzer, N. Miyakawa, K. E. Gray, D. G. Hinks, and C. Kendziora, Phys. Rev. Lett. **87**, 067005 (2001).

[17] J. Hwang, T. Timusk, and G. D. Hu, Nature (London) **427**, 714 (2004).

[18] T. Hasegawa, M. Nantoh, and K. Kitazawa, Jpn. J. Appl. Phys. **30**, L276 (1991).

[19] X. B. Zhu *et al.*, Phys. Rev. B **73**, 224501 (2006).

[20] R. Dipasupil, M. Oda, N. Momono, and M. Ido, J. Phys. Soc. Jpn. **71**, 1535 (2002).

[21] C. Kurter *et al.*, Phys. Rev. B **81**, 224518 (2010).

[22] K. A. Musaelian, J. Betouras, A. V. Chubukov, and R. Joynt, Phys. Rev. B **53**, 3598 (1996). In that work, and in the present, when the ratio of coupling constants c_Z/c_Δ is kept sufficiently small, a pure d-wave superconducting gap is justified.

[23] The identical tunneling matrix element has been used to calculate $I_C R_N$ for the junctions shown in this Letter (unpublished). The results obtained compare favorably with the measured $I_C R_N$ values in N. Miyakawa *et al.*, Phys. Rev. Lett. **83**, 1018 (1999) providing an independent check on the tunneling matrix element.

[24] E. van Heumen, E. Muhlethaler, A. B. Kuzmenko, H. Eisaki, W. Meevasana, M. Greven, and D. van der Marel, Phys. Rev. B **79**, 184512 (2009).

[25] J. Hwang, T. Timusk, E. Schachinger, and J. P. Carbotte, Phys. Rev. B **75**, 144508 (2007).

[26] P. D. Johnson, T. Valla, A. V. Fedorov, Z. Yusof, B. O. Wells, Q. Li, A. R. Moodenbaugh, G. D. Gu, N. Koshizuka, C. Kendziora, Sha Jian, and D. G. Hinks, Phys. Rev. Lett. **87**, 177007 (2001).

[27] T. Dahm *et al.*, Nature Phys. **5**, 217 (2009).